



ISSN: 2230-9926

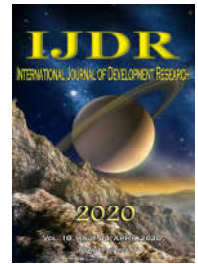
Available online at <http://www.journalijdr.com>

IJDR

International Journal of Development Research

Vol. 10, Issue, 08, pp. 38739-38743, August, 2020

<https://doi.org/10.37118/ijdr.19688.08.2020>



RESEARCH ARTICLE

OPEN ACCESS

DUAL-BAND PATCH ANTENNAS WITH CATACAUSTIC SLOTS FOR WIRELESS COMMUNICATION APPLICATIONS

Lamarks T. C. Cavalcanti^{1*} and Tales A. C. de Barros²

¹Graduate Program in Electrical Engineering, Federal Institute of Paraíba, João Pessoa - PB, Brazil

²Physics Department, State University of Paraíba, Patos - PB, Brazil

ARTICLE INFO

Article History:

Received 03rd May 2020

Received in revised form

11th June 2020

Accepted 17th July 2020

Published online 26th August 2020

Key Words:

Dual Antennas,
Patch Antennas,
Polar Elements,
Catacaustic Slots,
Wireless Communication.

ABSTRACT

It describes the development of antenna patches in microstrip with circular radiating elements defined in polar coordinates and catacaustic slots, which present multiband responses for application in wireless communications: cell phone communication, Wi-Fi and WiMAX. Inspired by the optical principle of caustic curves generated by reflection in the circumference, the catacaustic slots were introduced in patch antennas with these formats to tune their resonant properties. The proposed patch antennas were powered by microstrip lines with quarter-wave transformers for impedance adjustments. The antennas were designed with their irradiation and resonant properties analyzed precisely using the commercial software ANSYS Designer™. The experimental characterization of prototypes manufactured from patch antennas was carried out using a vector network analyzer. The agreement obtained between the simulated and measured results validated the adopted methodology and proved the frequency tuning property for multiband patch antennas studied.

*Corresponding author:

Lamarks T. C. Cavalcanti

Copyright © 2020, Lamarks et al. This is an open access article distributed under the Creative Commons Attribution License, which permits unrestricted use, distribution, and reproduction in any medium, provided the original work is properly cited.

Citation: Lamarks T. C. Cavalcanti and Tales A. C. de Barros. "Dual-Band Patch Antennas with Catacaustic Slots for Wireless Communication Applications", *International Journal of Development Research*, 10, (08), 38739-38743.

INTRODUCTION

Slots are used in radiating structures to allow greater versatility in antenna designs. Thus, applications in wireless communications operations in broadband, multiband, low and high frequencies can be improved. In this way, it is possible to manufacture antennas for applications in cell phone communication, WLAN, WMAN and promote the development of the area of wireless communications (Ali et al., 2013;Varma et al., 2017;Morshed et al., 2017). As well as mobile phone standards and laws, standards for wireless local area networks, WLAN, have also been developed. The operating standards for wireless local area networks were developed in the 1980s for ISM bands, but their use has increased since the 2000s for everyday use, due to improvements in Internet infrastructure and the advancement of telecommunications combined with decreased deployment costs. As a consequence, with the increase in connectivity and mobility of its users. The IEEE 802.11™ standard, WLAN, was used and continues to be widely studied, generating new applications, improvements in communications and security. In addition to energy savings in mobile or portable equipment (Khanna, 2008;Feng et al., 2017). In the same way as local networks, metropolitan wireless networks, WMAN, intend to provide wireless access to the Internet covering large areas. The term WiMAX was developed with the aim of promoting interoperability and compatibility between equipment that uses the IEEE 802.16™ standard (Chow et al., 2009;IEEE Std 802.16.1-2012;IEEE Std 802.16.1b-2012;IEEE 802.16.2-2004). However, the digital security of wireless networks has yet to be improved. Assuming that the signal propagates through the air in all directions when there are no blocking or guiding elements, wireless networks are vulnerable, whether in indoor or outdoor applications. For this reason, communications standards evolve according to need or are simply changed by amendments to address some lack of security.

And while wireless technologies are being perfected, handheld devices become smaller and operate more frequency bands. Like the cell phone, which was big and heavy at the beginning, working only for calls with analog technology. Currently, these devices have been reduced in size and present Wi-Fi, 3G, 4G, 5G, Bluetooth, GPS, NFC access, among other services. Thus, the need arises for antennas to operate in multiband, with the objective of saving internal space. The slots based on caustic curves have significant effects in controlling the resonant frequencies of antenna patches. With the contribution of geometric optics, it was possible to control resonance frequencies from slots in order to promote better frequency tuning in wireless communications.

THEORETICAL BACKGROUND

Caustic Curves: Caustic curves are generated by reflected or refracted rays of light. In which the envelope that defines the curve can be formed by shiny edges or shadows (Weistein, Beckman, 1970). When the envelope is generated by reflected rays, caustic curves are generated by reflections or catacaustic curves (Josse et al., 2012). Examples of catacaustic curves include cardioid, nephroid, logarithmic spiral, semicubic parabola, cubic Tschirnhausen, chase curve, as astroid and catenary, among others. Caustic refractive curves are also called diacaustic curves. In addition, there are orthocaustic curves, which the envelope is perpendicular to the radius emitted (Josse et al., 2012). Depending on how the light ray is reflected or refracted, places with a higher concentration of reflected rays may be formed, the cusp being an example. Its formation depends on the position of the focus of the light, the refractive index of the environments.

Cardioid Curves: Cardioid can be defined as an epicycloid curve between a fixed circumference of radius A and a rotating one, radius A , tangent to the fixed one. There is the presence of a cusp located at the origin of the cardioid curve (Josse et al., 2012). In addition, it is possible to form a cardioid curve from caustic curves from a circumference. When the focus of radiation is on the circumference, $\mu = A$, where A is the radius of the base circumference, a catacaustic curve in the form of a cardioid is generated (Josse et al., 2012). Figure 1 shows how it is formed from the catacaustic curve of the circumference (cardioid) from the tangency of reflected rays using the MATLAB™ software. Figure 2 highlights the catacaustic curve of the circumference, cardioid, with the respective cusp being the point with the highest concentration of rays per area.

Circular Patch Antennas with Catacaustic Slot: Circular patch antennas have a predominant dual band behavior, with a tendency to generate few frequencies of unwanted resonances. In addition to having the advantage of being reduced in size. The parametric equations that describe the circular patch are described by 1 and 2, where A is the radius of the base circumference. In the y direction, an offset equal to the radius is applied.

$$x_{cir} = A \cos(t) \quad (1)$$

$$y_{cir} = A \sin(t) + A \quad (2)$$

$$x_{1.slot.car} = 2A \sin(t)(1 + \cos(t))/3 \quad (3)$$

$$y_{1.slot.car} = -6A \cos(t)(1 + \cos(t)) + 4A/3 \quad (4)$$

$$x_{2.slot.car} = 2(A - w_s) \sin(t)(1 + \cos(t))/3 \quad (5)$$

$$y_{2.slot.car} = -6(A - w_s) \cos(t)(1 + \cos(t)) + 4(A - w_s)/3 \quad (6)$$

Figure 3 illustrates an example of a patch antenna generated by software when joining patch, slot, defined by Equations 3, 4, 5 and 6, with the quarter wave transformer an example of a circular patch antenna with catacaustic slot is obtained for simulation. To calculate the length of the slot catacaustic curve, it is used Equations 7 and 8.

$$dl = \sqrt{dx(t)^2 + dy(t)^2} \quad (7)$$

$$dl(t) = \int_a^b dl \quad (8)$$

METHODOLOGY

Figure 4 presents a block diagram that summarizes the adopted methodology. The antenna layouts for polar patches are made using mathematical modeling of the radiating patch geometry, the catacaustic slot of the respective polar curves and the feed line, which are designed with the aid of MATLAB™. The code is executed in the MATLAB™ software for circular patch antennas. As code inputs, there is the radius A of the base circumference of the structure that generates each of the radiating elements, the width W_{qwt} and length L_{qwt} of the quarter-wave transformer used to make the impedance adjustments. In addition to the slot opening angle, $2\pi/\theta_s$. The first type of file is formed by the union of the radiating element, quarter-wave transformer and microstrip line. In which the radiating element derived from the base circumference defined by variable A . The second type is the slot file, which refers to the catacaustic curve of the original radiating element. And finally, the third type of file is composed of a rectangle that defines the ground plane of the patch antenna. Datas are exported to the ANSYS Designer™ software, where the simulation is performed using the design parameters within the limitations required for each structure. For cardioid and circular

patch antennas. The simulations results of modules of reflection coefficients are performed from 1 to 7 GHz, interpolated and sampled every 1 MHz. While the simulated results of current density distribution use discrete analyzes at the desired frequencies. After this procedure, if the result meets the resonance frequencies, the bandwidth of interest and the reflection coefficient module, the data is exported to the manufacturing in FR4, with $\epsilon_r = 4.4$. The measurements are made with the antenna manufactured in the laboratory. The measured results are recorded in files with graphs and spreadsheet analysis. Finally, it is decided whether the validity of the antenna interests them.

RESULTS

Design Parameters for Circular Patch Antennas: As circular patch antennas present a greater limitation for tuning resonance frequencies, circular antenna designs have greater variations in parameters. It is necessary to adjust the sizes of radius A of the base circumference. The quarter-wave transformer is defined by two variables, width W_{qwt} and length L_{qwt} . The slot has three associated variables. The first is the opening angle $2\pi/\theta_s$; the second is the length $L_{slot.car}$ and w_s , which is the difference between the base circumference of radius A and a second tangential circumference with the radius equal to $A - w_s$. Table 1 shows the parameters used in projects A and B.

Table 1. Parameters for circular patch antenna designs

	Projeto A	Projeto B
A (mm)	12.34	11.65
$L_{slot.car}$ (mm)	0.00	30.26
$2\pi/\theta_s$ (rad)	$+\infty$	2.10
L_{qwt} (mm)	9.50	8.15
W_{qwt} (mm)	0.53	0.46
w_s (mm)	0.60	0.60

Table 2. Frequency ratios in percentage for circular patch antennas for $A = 10$ mm

θ_s	4.4	3.4	2.4	1.4
$2\pi/\theta_s$ (rad)	1.43	1.85	2.62	4.49
L_{slot} (mm)	18.08	23.06	31.50	46.61
Res. Freq. 1 - $A = 10$ mm (%)	99.83	99.07	92.60	64.92
Res. Freq. 2 - $A = 10$ mm (%)	99.93	99.31	99.32	79.41

Circular Patch Antennas: Project A: The circular patch antenna without slot for Project A has the goal to obtain the 5 GHz Wi-Fi band and present the dual band behavior of the antenna. The radius of the radiating element A is 12.34 mm, while the quarter-wave transformer has a length, L_{qwt} , equal to 9.5 mm and a width, W_{qwt} , of 0.53 mm, shown in Table 1. Figure 5 illustrates the antenna manufactured and which was used to make the measurement in the laboratory. Figure 6 shows the comparison between the simulated and measured results of the circular patch antenna without slot designed for 5 GHz band of Project A. The measurement in the laboratory confirms the simulation, when the comparison between the two curves is performed. The first one occupies the band from 3.32 to 3.41 GHz, with a bandwidth of 90 MHz and resonance at 3.36 GHz. However, this band does not belong to WiMAX 3.5 GHz, whose range band is from 3.4 to 3.6 GHz. Figure 7 presents the simulated current density distribution of Project A for 3 GHz band. The distribution behaves with a tendency of homogeneity in the radiating element. The simulated 2D irradiation pattern of Project A for the 3 GHz band is shown in Figure 8. Only a unique frontal and posterior lobe is formed. Figure 9 shows the 3D irradiation diagram of Project A for the 3 GHz band. It is possible to observe the main frontal and posterior lobes without irregularity in the irradiated field, besides presenting bilateral symmetry. The maximum gain of the antenna is 6.80 dB. The second band occupies the 5 GHz Wi-Fi band. The minimum frequency is 5.46 GHz and the maximum is 5.57 GHz, with a bandwidth of 105 MHz. Resonance occurs at the frequency of 5.52 GHz.

Figure 10 illustrates the current density distribution of the circular patch antenna for 5 GHz Wi-Fi band of Project A. The center of the antenna has minimum current density values that increase towards the edges of the radiating element. The 2D radiation pattern of Project A of the circular patch antenna without slot for 5 GHz Wi-Fi band is illustrated in Figure 11. Due to the minimum value of the current density in the center of the radiating element, the diagram antenna irradiation has multiple lobes slightly irregular, but bilaterally symmetrical. Figure 12 shows the 3D radiation pattern of Project A simulated for 5 GHz band. The irradiation is bilaterally symmetrical. However, due to the influence of the current density distribution, the lobe that radiates from the bottom of the antenna is deformed when compared to the one that radiates towards the lobe that radiates to the top of the radiating element.

Circular Patch Antennas: Project B: The slotted circular patch antenna of Project B has applications for 3.5 and 5 GHz band. The radiating element has a radius, A , equal to 11.65 mm. In addition to presenting a catacaustic slot in length, $L_{slot.car}$, equal to 30.26 mm, generated by an opening angle, $2\pi/\theta_s$, of 2.09 rad. Finally, the quarter-wave transformer has a length, L_{qwt} , equal to 8.15 mm and a width, W_{qwt} , with a value of 0.46 mm. Figure 13 illustrates the antenna manufactured with a slotted circular patch for 3.5 and 5 GHz with the layout designed by MATLAB™. Figure 14 shows the comparison between the simulated and measured

results of the slotted circular patch antenna designed for frequency bands of 3.5 GHz and 5 GHz. The manufactured antenna is similar in response to the simulated antenna. It also presents, in addition to presenting values under -17.5 dB for values of the reflection coefficient module, $|\Gamma_{11}|$, for the first two resonance frequencies. The WiMAX 3.5 GHz bandwidth is 90 MHz for Project B, with a minimum frequency of 3.43 GHz and a maximum frequency of 3.52 GHz. The resonance frequency is 3.48 GHz. And for 5 GHz Wi-Fi band, the resonant frequency is 5.74 GHz. The bandwidth is 90 MHz, from 5.70 to 5.79 GHz. Figure 15 illustrates the current density distribution of Project B simulated of the slotted circular patch antenna for WiMAX 3.5 GHz band. The highest current density intensities in the radiating element are at the edges of the slot. The 2D radiation pattern of Project B simulated for WiMAX 3.5 GHz band is shown in Figure 16. Two regular lobes are visible.

Figure 17 illustrates the 3D radiation pattern simulated of the slotted circular patch antenna for 3.5 GHz band in Project B. The maximum gain of 5.83 dB pointing to the front of the antenna. Figure 18 shows the current density distribution simulated of the slotted circular patch antenna for 5 GHz band in Project B. A point of minimum current density distribution is found near the center of the radiating element. And the highest current densities in the radiating element are found at the edges of the slot. The 2D radiation pattern of Project B simulated of the slotted circular patch antenna for 5 GHz band is shown in Figure 19. As expected by the current density distribution, the irradiation lobes formed are irregular. And Figure 20 is shown the 3D radiation pattern of Project B simulated of the slotted circular patch antenna for 5 GHz Wi-Fi band. There is an irregular frontal lobe radiating mainly to the sides of the antenna, upside and downside, where the highest gain value is 6.11 dB.

Parametric Analysis of Slotted Patch Antenna: To understand how the slot behavior in the circular patch antennas is carried out, a series of controlled simulations were performed in ANSYS Designer™. The only parameter changed was the slot size, keeping the others constant. For this result evaluation, one point was considered every 1 MHz and using interpolation method. The θ_s value is between 1.2 and 5.0. It is known that smaller the slot is, greater the value of θ_s and the increase in the value of θ_s generates an increase in frequencies.

Parametric Analysis of Circular Patch Antennas for $A = 10$ mm: It is considered that $A = 10$ mm, $W_{qwt} = 0.67$ mm, $L_{qwt} = 7$ mm and $w_s = 0.6$ mm. These antennas are more stable and present fewer resonance frequencies. Presenting three noticeable resonance frequencies with a predominance of dual band behavior, as shown in Figure 18. Figures 21a, 21b and 21c shows the comparison of slot sizes for circular patch antennas designed with the aid of MATLAB™ for $A = 10$ mm used in parametric analysis. For lower frequencies, a slot equivalent to $\theta_s = 1.2$ has 44.05% of the antenna without slot and with 4.8, it has 99.90%. While the upper frequency, it presents 73.21% and 99.93% of the upper frequency with no slot. The resonance frequencies, considering dual band, of the antenna without slot are 4.08 and 6.71 GHz, respectively. Figure 22 illustrates the parametric analysis of the resonance frequencies of the smaller circular patch antennas as a function of the length of the catacaustic (cardioid) slot for values of $A = 10$ mm, $W_{qwt} = 0.67$ mm, $L_{qwt} = 7$ mm and $w_s = 0.6$ mm. When the length of the slots is between 30 and 40 mm, the slope of the analysis curve for second strip changes. Equivalent to a θ_s ranging from 1.8 and 2.6. Thus, it was necessary to carry out further testing to confirm whether the result is valid or an error. Table 2 shows the frequency ratios in percent for circular patch antennas for $A = 10$ mm. Only the first two frequency bands are analyzed due to their stability. For values of θ_s greater than 4.4, or $2\pi/\theta_s$ less than 1.43 rad, the presence of the catacaustic slot does not present a considerable difference compared to the antenna without the presence of the slot.

Conclusion

This paper discussed the behavior of circular patch antennas with their respective slots generated from catacaustic curves. All antenna layouts were generated using MATLAB™. The circular patch antennas with catacaustic slots (cardioid curves) have the advantage of having a smaller size. In addition, the impedance adjustment is simple, as the dual band behavior is maintained. However, tuning specific bands is more complicated than in cardioid patch antennas and simpler than in nephroid patch antennas. The two resonance frequencies change with the change in the size of the cardioid slot. Another point is that the radiation pattern of the patch antennas can change with the presence of catacaustic slots. This occurs mainly from the second frequency range. It is concluded that the structures, properly with their catacaustic slots, detailed here present as a tool for frequency tuning. This facilitates designs for applications for multifunction antennas. It can be applied to mobile communication, Wi-Fi and WiMAX technologies and communications on portable devices. In addition, the quarter-wave transformer can be used to privilege a frequency or a group of frequencies and the structure of the radiating element is maintained.

Acknowledgement

The authors would like to thank the Federal Institute of Paraíba (IFPB) for help and access to used equipment.

REFERENCES

- Ali, M. et al. A Dual Band U-Slot Printed Antenna Array for LTE and WiMAX Applications. *Microwave and Optical Technology Letters*, v. 55, n. 12, p. 2879–2883, 2013.
- Chow, B. et al. Radio-over-fiber distributed antenna system for wimax bullet train field trial. In: 2009 IEEE Mobile WiMAX Symposium. Napa Valley, CA, Estados Unidos: IEEE, 2009. p. 98–101.
- Feng, Y. et al. IEEE 802.11 HCCA for tactile applications. In: 2017 27th International Telecommunication Networks and Applications Conference (ITNAC). Melbourne, VIC, Austrália: IEEE, 2017. p.1–3. ISSN 2474-154X.

- IEEE. IEEE Recommended Practice for Local and Metropolitan Area Networks Coexistence of Fixed Broadband Wireless Access Systems. IEEE Std 802.16.2-2004 (Revision of IEEE Std 802.16.2-2001), p. 1–166, Mar. 2004.
- IEEE. IEEE Standard for WirelessMAN-Advanced Air Interface for Broadband Wireless Access Systems Amendment 1: Enhancements to Support Machine-to-Machine Applications. IEEE Std 802.16.1b-2012 (Amendment to IEEE Std 802.16.1-2012), p. 1–126, Oct. 2012.
- IEEE. IEEE Standard for WirelessMAN-Advanced Air Interface for Broadband Wireless Access Systems. IEEE Std 802.16.1-2012, p. 1–1090, Set. 2012.
- IEEE. IEEE Standard for WirelessMAN-Advanced Air Interface for Broadband Wireless Access Systems - Amendment 2: Higher Reliability Networks. IEEE Std 802.16.1a-2013 (Amendment to IEEE Std 802.16.1-2012), p. 1–319, Jun. 2013.
- Josse, Alfrederic, Pène, Françoise. On the class of caustics by reflection, 2012. Available in: <www.researchgate.net/publication/232642424_On_the_class_of_caustics_by_reflection>. Access: 3 Dec 2019.
- Khanna, V. K. Designing low power ad-hoc 802.11 wireless networks for voice and video applications. In: TENCON 2008 - 2008 IEEE Region 10 Conference. Hyderabad, India: IEEE, 2008. p.1–6. ISSN 2159-3442.
- Morshed, K. M.; Karmokar, D. K.; Esselle, K. P. Low profile single-layer U-slot loaded shorted-patch antenna for wireless communications. Microwave and Optical Technology Letters, v. 59, n. 9, p. 2224–2226, 2017.
- Varma, R.; Ghosh, J.; Bhattacharya, R. A compact dual frequency double U-slot rectangular microstrip patch antenna for WiFi/WiMAX. Microwave and Optical Technology Letters, v. 59, n. 9, p. 2174–2179, 2017.
- Weinstein, L. A.; Beckman, P. Open resonators and open waveguides. *American Journal of Physics*, v. 38, p. 114–115, Jan 1970.
